JBC Papers in Press. Published on July 13, 2010 as Manuscript M110.129577
The latest version is at http://www.jbc.org/cgi/doi/10.1074/jbc.M110.129577

Essential molecular determinants for thyroid hormone transport and first structural implications for monocarboxylate transporter 8

[1]Anita Kinne*, [2,3]Gunnar Kleinau*, [1]Carolin S. Hoefig, [2]Annette Grüters, [1]Josef Köhrle, [3]Gerd Krause, [1]Ulrich Schweizer

[1]Institut für Experimentelle Endokrinologie, [2]Institut für Experimentelle Pädiatrische Endokrinologie, Charité-Universitätsmedizin Berlin, Germany, [3]Leibniz-Institut für Molekulare Pharmakologie, Berlin, Germany

Running head: Structure-function relationships in MCT8

* equal contribution

Address correspondence to: Dr. Ulrich Schweizer, Institut für Experimentelle Endokrinologie, Charité-Universitätsmedizin Berlin, Augustenburger Platz 1, 13353 Berlin; Phone: ++4930450524080; Fax: ++49 30 450 524 922; email: ulrich.schweizer@charite.de

Monocarboxylate transporter 8 (MCT8, SLC16A2) is a thyroid hormone (TH) transmembrane transport protein mutated in Allan-Herndon-Dudley syndrome, a severe X-linked psychomotor retardation. The neurological and endocrine phenotypes of patients deficient in MCT8 function underscore the physiological significance of carrier-mediated TH transmembrane transport. MCT8 belongs to the major facilitator superfamily of 12 transmembrane spanning proteins and mediates energy-independent bidirectional transport of iodothyronines across the plasma membrane. Structural information is lacking for all TH transmembrane transporters. In order to gain insight into structure-function relations in TH transport, we chose human MCT8 as paradigm. We systematically performed conventional and liquid chromatography-tandem mass spectrometry-based uptake measurements into MCT8-transfected cells using a large number of compounds structurally related to iodothyronines. We found that human MCT8 is specific for L-iodothyronines and requires at least one iodine atom per aromatic ring. Neither thyronamines, decarboxylated metabolites of iodothyronines, nor triiodothyroacetic acid and tertraiodothyroacetic acid, TH derivatives lacking both chiral center and amino group, are substrates for MCT8. The polyphenolic flavonoids naringenin and F21388, potent competitors for TH binding at transthyretin, did not inhibit T_3 transport, suggesting that MCT8 can discriminate its ligand better than transthyretin. Bioinformatic studies and a first molecular homology model of MCT8 suggested amino acids potentially involved in substrate interaction. Indeed, alanine mutation of either Arg445 (helix 8) or Asp498 (helix 10) abrogated T_3 transport activity of MCT8, supporting their predicted role in substrate recognition. The MCT8 model allows to rationalize potential interactions of amino acids including those mutated in patients with Allan-Herndon-Dudley syndrome.

Thyroid hormones (TH)[1] are amino acid derivatives. Owing to their zwitter-ionic nature, TH and their derivatives require transmembrane transporters to mediate their translocation across the plasma membrane (1). Several classes of transmembrane transporter proteins of the major facilitator superfamily (MFS) are capable of TH transport: organic anion transporters two and three (Oatp2 and Oatp3) were the first TH transporters cloned (2). Later, L-type amino acid transporters (Lat1, Lat2) (3) and monocarboxylate transporters eight and ten (MCT8 and MCT10) were shown to transport TH (4;5). Among these transporters, only MCT8 is specific for TH. Mutations in MCT8/SLC16A2 lead to severe psychomotor retardation and TH abnormalities in humans (6;7), including the Allan-Herndon-Dudley Syndrome (8). Patients suffering from mutations in MCT8 are characterized by high serum T_3 values associated with low T_4 and inappropriately normal TSH. This clinical phenotype suggested that MCT8 is involved in pituitary feedback control of

the TH axis. Sensitivity to TH thus depends on the expression of TH transporter molecules. Expression of MCT8 in the mouse brain (9) supported the idea that TH import into neurons may be affected in patients afflicted with the Allan-Herndon-Dudley syndrome. Mice deficient in MCT8 recapitulate the disturbed serum thyroid hormone parameters (10;11), but exhibit only mild neurological abnormalities (12). Murine neurons are apparently protected from the lack of MCT8 by expression of alternative T_3 transporters such as Lat2, which is not present in human developing neurons (12).

More than two-dozen mutations in MCT8 have been identified in human patients (13). Genotype-phenotype correlations suggested that most missense mutations cause a complete loss-of-function phenotype in patients. A comparison of 12 missense mutants revealed that pathogenic MCT8 mutations may affect expression, surface translocation or specifically the substrate transport mechanism (14). Possibly, homodimerization may also play role which we currently do not understand (15;16). To our knowledge, no data are yet available relating structural features and transport mechanism of MCT8.

Our goal in this study was to obtain new functional and structural insights in the complex system of substrate binding and transport. Systematic analysis of substrate molecules for MCT8-mediated cellular uptake revealed several structural determinants for substrate recognition by MCT8: an L-amino acid side chain and at least an iodine substitution in the 3 positions of both aromatic rings of the thyronine moiety. We also designed a homology model of human MCT8 to identify amino acids potentially involved in substrate recognition. Strikingly, mutations of charged amino acids predicted to interact with substrate disrupted T_3 import into cells. Thus, functional data support the first predictions from our structural MCT8 model.

EXPERIMENTAL PROCEDURES

Site-directed mutagenesis and stable cell lines

Mutations were introduced into human MCT8 by overlap extension PCR with the following primers (mutated bases in bold-face) R445A-fwd 5`-CAGGCCTTGGG**GCT**CTTGTGTCAGGCCAC-3`, R445A-rev 5`-GTGGCCTGACACAAG**AGC**CCCAAGGCCTG-3`, D498A-fwd 5`-CTGGGCCTTTGC**GCC**GGCTTCTTCATCAC-3` and D498A-rev 5`-GTGATGAAGAAGCC**GGC**GCAAAGGCCCAG-3`. Plasmids were stably transfected into MDCK1 cells as described previously (14).

T_3 uptake assays

One day before the experiments, 200,000 cells per well were seeded into 12-well plates. ^{125}I-T_3 (Perkin Elmer) was purified from iodide ions by adsorption chromatography and finally resuspended in DMEM-F12 (1:1) without serum (14). For competitive inhibition studies, cells were exposed to 10 nM ^{125}I-T_3 tracer in medium for three minutes in the presence or not of 10 µM of test compound (1 mM for aromatic amino acids and BSP), medium was removed and radioactivity associated with the cells determined (supplemental Fig. S2). Iodothyronines and related compounds were first dissolved in DMSO (1000-fold final concentration), and then in medium. Aromatic amino acids were dissolved in uptake buffer (125 mM NaCl, 5 mM KCl, 1.3 mM $CaCl_2$, 1.2 mM $MgCl_2$, 25 mM HEPES, 5.6 mM glucose, pH 7.4). For time course assays, stably transfected cell lines were incubated with 10 nM tracer for 1 to 30 minutes. After a single wash with ice cold PBS, cells were lysed in 40 mM NaOH, and radioactivity of the lysate was measured in a gamma counter (Wizard, Perkin Elmer). Each experiment was performed on at least two different days with different batches of cells in triplicate. Radioactivity associated with empty vector-transfected cells was subtracted as background and the activity associated with the wildtype MCT8 clone without inhibitor was defined as 100%.

For determination of apparent K_M values of wildtype MCT8, MDCK1 cells were incubated for three minutes with T_3 at concentrations ranging from 500 nM to 12 µM containing or not ^{125}I-T_3 as tracer. A Michaelis-Menten transport mechanism was assumed for calculations (GraphPad 4.0). Iodothyronines were supplied by Formula GmbH (Berlin, Germany), thyronamines were kindly provided by Dr. Thomas Scanlan (Portland, USA) and F21388 by Prof. Schreier (Würzburg, Germany). TRIAC and TETRAC were obtained from Henning (Berlin, Germany) and naringenin was purchased from Sigma-Aldrich (Taufkirchen, Germany).

The uptake of T_3, T_3AM, and TRIAC by wildtype MCT8 and the mutants R445A and D498A was directly measured by LC-MS/MS (17;18). The cells were incubated for three minutes in DMEM-F12 (1:1) with a final concentration of 50 µM. Then the medium was removed and cells washed once with ice cold PBS and harvested.

Liquid chromatography-tandem mass spectrometry (LC-MS/MS)-Instrumentation and Detection

LC-MS/MS analyses were performed using a Shimadzu UFLC system (Shimadzu Scientific Instruments, Columbia, MD) and a 4000QTRAP triple-quadrupole tandem mass spectrometer (Applied Biosystems, Darmstadt, Germany) equipped with TurboIonSpray interface. The chromatographic column and the autosampler were operated at 40 °C and 10 °C, respectively. The detection was performed using positive electrospray ionization (ESI+) for T_3 and T_3AM and negative electrospray ionization (ESI-) for TRIAC in the selected reaction monitoring (SRM) mode. The mass spectrometric working parameters were: TurboIon spray voltage (IS): 5500 V, curtain gas (CUR): 30 psi, collision gas (CAD): 5 psi, nebulizer gas (GS1): 60 psi, heater gas (GS2): 50 psi, entrance potential (EP): 10 V, source temperature: 400 °C, dwell time: 90 ms.

Chromatographic separation of all substances was achieved using a Synergi Polar-RP 80-Å column (150 x 2 mm; Phenomenex, Aschaffenburg, Germany) and an analytical Guard Cartridge System (4.0 mm x 2.0 mm, Phenomenex, Aschaffenburg, Germany) using a gradient elution program at a flow rate of 300 µl/min. Simultaneous detection of all substances in the same biological sample was performed using a modified LC-MS/MS method as described before (18). With the 4000QTRAP triple-quadrupole tandem mass spectrometer we reduced the time per run to 25 min using a gradient elution program: 0–2 min, 2% B; 2–12 min, 40% B; 12–15 min, 60% B; 15–15.5 min, 90% B; 15.5–16.5 min, 90% B; 16.5–17 min, 2% B; 17–19.95 min, 2% B. The device-specific mass spectrometric parameters for analytes are presented in table 1. Data processing was performed using Bio Analyst version 1.5. Software (Applied Biosystems, Darmstadt, Germany). Liquid-liquid extraction of all compounds for LC-MS/MS analysis was performed as described previously (17). For LC-MS/MS analysis 4 pmol deuterated 3-T_1AM-d_4 was used as internal standard (IS).

Surface biotinylation and Western blotting

Surface biotinylation was performed on MDCK1 cells as previously described (14). Briefly, equal amounts of 5 µg of biotinylated protein (or 80 µg of total cellular protein fraction) were separated on SDS gels, transferred onto nitrocellulose membranes, and probed with an MCT8 antibody (Atlas, Stockholm, Sweden). An antibody directed against β-actin (Rockland, Gilbertsville, USA) was used for loading control. Every experiment was performed at least twice with similar results.

Bioinformatics and molecular homology modeling

All amino acid sequence alignments (Fig.1 and supplemental Fig. S1) were produced using a combination of automatic and manual procedures. For automatic alignments, ClustalW (19) software was applied with the Blossum62 amino acid similarity matrix. Few manual refinements were performed including Gap-introduction at loop regions, but not in transmembrane helices. Alignments were produced with the *BioEdit* software package (http://www.mbio.ncsu.edu).

Human MCT family members were aligned to analyze shared and divergent features in amino acid composition (Fig. 1). The potential dimensions of transmembrane helices (TMH) were predicted based on observable helices in the crystal structure of the Glycerol-3-phosphate transporter (GlpT, PDB code 1PW4 (20)), another member of the MSF superfamily (supplemental Fig. S1) which can be used as a structural template for homology models (see section below). From this alignment it becomes obvious, that MCT family proteins share high sequence and most likely structural similarity, despite some regions of flexibility like the third intracellular loop (ICL3).

The high sequence similarity among MCT proteins suggested to us to propose a unifying numbering system for this protein subfamily. The rationale of this numbering scheme is adopted from the description by Ballesteros and Weinstein for family A G-protein-coupled receptors (GPCR) (21). We use the numbering convention x.50 for the most conserved amino acids in each transmembrane helix (TMH) x. For example, the most highly conserved residue in TMH1 is defined as 1.50 and in TMH2 as 2.50 etc.. We suggest the following amino acids as highly conserved for all MCT (Fig. 1): $W^{1.50}$ (MCT8

W175) at TMH1, TMH2 $P^{2.50}$ (MCT8 P233), TMH3 $G^{3.50}$ (MCT8 G258), TMH4 $G^{4.50}$ (MCT8 G276), TMH5 $G^{5.50}$ (MCT8 G312), TMH6 $G^{6.50}$ (MCT8 S351), TMH7 $P^{7.50}$ (MCT8 P412), TMH8 $R^{8.50}$ (MCT8 R445), TMH9 $G^{9.50}$ (MCT8 G472), TMH10 $G^{10.50}$ (MCT8 G499), TMH11 $P^{11.50}$ (MCT8 P536), TMH12 $F(Y)^{12.50}$ (MCT8 F554).

The crystal structure of the inward facing conformation of GlpT from *Escherichia coli* was used as a structural template for a MCT8 homology model (20). The alignment between human MCT8 and GlpT amino acid sequences reveals a similarity score of 25.5% (supplemental Fig. S1). With small deviations, the helix dimensions observed in the GlpT crystal structure are applicable for human MCT8. The reliability of this structural template is supported by examples of modeling for other members of the MFS like GLUT1 (22) or MCT1 (23;24). Helices in MCT8 comprise the following residues: TMH1 F166-L202, TMH2 Q212-T239, TMH3 C244-H260, TMH4 R271-H296, TMH5 Q299-M326, TMH6 T336-T353, TMH7 G401-E429, TMH8 V435-L458, TMH9 I461-M477, TMH10 F484-L512, TMH11 A521-G548, and TMH12 A553-D589.

Gaps of missing residues in the loops of the template structure were closed by the 'Loop Search' tool implemented in Sybyl 7.35 (Tripos Inc., St. Louis, MO, USA). Comparison to loop conformations extracted from the PDB by the *Super-Looper* software (http://bioinformatics.charite.de/superlooper/index.php) were also performed to find superimposing loop-structures from the PDB as criteria for reliability. The quality and stability of the model were validated by checking the geometry using PROCHECK (25).

Side-chains and loops of the homology model were subjected to conjugate gradient minimization (until converging at a termination gradient of 0.05 kcal/(mol*Å)) and molecular dynamics simulation (5 ns) by fixing the backbone H-bonds of the TMH. Finally the model was minimized without any constraints.

Structure images were produced using *PyMOL* software (DeLano WL, version 0.99, San Carlos, CA, USA (http://www.pymol.org)).

RESULTS

Structural determinants of substrate molecules determined by competition with ^{125}I-T_3

The only substrates of MCT8 so far identified are iodothyronines (4). A large number of iodothyronines and related molecules are available to probe structural determinants for transport by MCT8. The basic structure of thyroid hormones is the thyronine backbone carrying iodine atoms at one or several of four possible positions (Fig. 2*A*). The thyroid produces mainly 3,3',5,5'-tetraiodo-L-thyronine (thyroxine, T_4) which can be converted by the action of iodothyronine deiodinases into any iodothyronine (26). Moreover, thyronamines (TAM), decarboxylated iodothyronine derivatives, and iodothyroacetic acids are naturally occurring metabolites and exert biological and pharmacological effects (27;28). We tested a total number of twenty-three iodothyronine derivatives for their interference with transport of the paradigmatic MCT8 substrate, T_3. Among L-(iodo)thyronines, only T_4, T_3, rT_3, and 3,3'-diiodothyronine (3,3'-T_2) competed with T_3 for transport (Fig. 2*B*). We concluded that MCT8 requires for transport at least one iodine atom at the 3 positions in both aromatic rings.

In addition, L-T_3 transport is inhibited only by L-iodothyronines, while their D-isomers had no effect (Fig. 2*C*). These results support and extend similar studies of rat Mct8 by Friesema (4).

We then asked whether TAM, also compete with T_3 for transport by MCT8. In comparison with L-iodothyronines, TAM lack the amino acid carboxyl group and the chiral center.

Inhibition by a 1000-fold excess of any TAM was negligible with the single exception of 3-iodothyronamine (3-T_1AM), an endogenous metabolite known to exert profound pharmacological effects (27;29). But even at 10 µM, 3-T_1AM achieved a maximal inhibition of only about 30% of T_3 uptake (Fig. 2*D*) (30).

Our next question was whether the amino group of the backbone represents an important structural determinant. In contrast to earlier findings with rat Mct8 (4), N-acetylation of iodothyronines is apparently tolerated by human MCT8, since NAc-T_3 and NAc-T_4, both exhibited inhibitory effects similar to the non-acetylated compounds (Fig. 2*E*). TRIAC and TETRAC were entirely devoid of inhibitory potential in the competition assay (Fig. 2*E*).

Our conclusions regarding substrate recognition were supported by the lack of inhibition by 3,5-diiodo-thyropropionic acid (DITPA, see Fig 2*E*), a

thyromimetic compound which was used to pharmacologically circumvent the transport deficiency in *Mct8*-deficient mice (31). Unlike the closely related MCT10, MCT8 does not accept aromatic amino acids (Fig. 2*F*).

Finally, we tested polyphenolic flavonoids F21388 and naringenin for inhibition of T_3 transport. These compounds were previously shown to bind to transthyretin and compete for T_4 binding. Both flavonoids were inactive in this uptake assay in contrast to the known MCT8 inhibitor, bromosulphtalein (BSP, Fig. 2*G*) (4).

Measuring the uptake of MCT8 substrates with LC-MS/MS

Competition assays are an easy and common way to determine structural determinants for receptor binding or transport. However, this type of experiments represents an indirect approach. We took advantage of our LC-MS/MS assays for iodothyronines and TAM (17;18) and directly measured uptake of unlabelled ligands into MCT8-transfected MDCK1 cells. In a first step, we validated the LC-MS/MS method in direct comparison with the established ^{125}I-T_3 uptake assay (Fig. 3*A* and *B*). The K_M values determined by both methods, 4.7 µM and 7.5 µM, are within the range reported for rat, 4-8 µM (4). We then tested T_3AM and TRIAC. Even at 50 µM, both compounds were not transported by MCT8 (Fig. 3*C*). Thus, the direct assay supports that MCT8 requires the intact L-amino acid backbone for substrate recognition.

Two charged amino acids are spatially located at the potential substrate transport channel

We were interested in the identification of amino acids in MCT8, which are involved in substrate recognition. Structure-function analysis of the substrate suggested a requirement for both amino and carboxylic functional groups. Therefore, we focussed on charged amino acids located in the transmembrane helices. The MCT sequence alignment revealed that all MCTs carry a conserved arginine in TMH8 (R445, position 8.50). In MCT1, the corresponding amino acid (R306) is described to be essential for transporter function (23). We built a homology model for MCT8 based on the X-ray structure of GlpT (Fig. 4*A*). Our model is in a conformation open to the intracellular side (Fig. 4*B*). In this model the charged side chain R445 points into the interior space between the transmembrane helices. Moreover, R445 protrudes into a solvent filled cavity, which we presume is the substrate channel (Fig. 4*B*). This arginine likely interacts within the interior region of the transporter with a negative charge from the substrate. The MCT8 model further suggests a salt bridge between R445 and D498 (TMH10). Thus, both charged residues might be involved in essential helix interactions or in substrate recognition.

Mutations in R445 and D498 lead to total loss of transport activity

In order to test the significance of the two charged amino acids, R445 and D498, for substrate transport, we replaced both amino acids with alanine, established stable cell clones and tested their activity. Alanine replacement removes charges while retaining the propensity of a peptide to form helices. Both mutants were expressed at lower levels than wildtype, but were exposed to the plasma membrane as shown by surface biotinylation (Fig. 5*A*). Strikingly, both mutants entirely lacked any ^{125}I-T_3 uptake activity (Fig. 5*B*). If the functional role of these charged amino acids relied solely on interaction with the amino acid backbone of the iodothyronine substrate, alanine mutants should accept T_3AM or TRIAC at least at high concentration. We tested this hypothesis directly using the LC-MS/MS assay. Both alanine mutations entirely abrogated transport of T_3 and the mutant MCT8 did neither accept TRIAC nor T_3AM (Fig. 5*C*). This finding is compatible with the assumption that an essential salt-bridge between basic R445 and acidic D498 may be formed during the transport cycle.

DISCUSSION

As a first step to gain insight into structural features, substrate interaction, and transport mechanism of thyroid hormone transporters, we systematically delineated the conserved structural elements in MCT8 substrates and tried to identify amino acids in MCT8 potentially interacting with substrate. A homology model for MCT8 was built based on the structure of GlpT, a bacterial Glycerol-3-phosphate transporter (20). Combining modelling and biochemical approaches, we identified two essential charged amino acids in TMH8 and TMH10 located in close proximity to the presumed substrate transport channel.

Substrate determinants required for recognition by MCT8

Using 23 iodothyronine and related compounds, we systematically investigated their structure function relationships to extract key features of MCT8 substrates. Unlike MCT10 (4;5), MCT8 does not transport aromatic amino acids, suggesting specificity for the thyronine structure. Moreover, human MCT8 is sensitive to the number and distribution of iodine atoms attached to the thyronine backbone. Our data support and extend earlier work done in Xenopus oocytes (4) and show that MCT8 substrates have to carry at least an iodine atom in the 3 positions of both aromatic rings. In addition, an L-amino acid moiety is essential. In contrast to the findings on rat Mct8 expressed in Xenopus oocytes (4), human MCT8 expressed in MDCK1 cells tolerated N-acetylation of iodothyronines, and was not inhibited by D-isomers and TRIAC. Neither naringenin nor F21388 interfered with T_3 transport by MCT8. Hence, MCT8 has higher specificity for iodothyronines than type I-deiodinase (32-34), transthyretin (32), and T_3-receptors (35;36).

Amino acids in MCT8 involved in both substrate recognition and transport

Our alignment of MCT family amino acid sequences revealed R445 (position 8.50) as conserved among all MCT family proteins (Fig. 1). This high conservation indicates an important and specific function for this amino acid and indeed, in our homology model, R445 protrudes into a central cavity in the protein in between the helices (Fig. 4*B*), which we assume is representing the substrate channel in accordance with the GlpT structure (20). This channel assignment is in agreement with the hypothesis that cavities within membrane gates are encircled by polar amino acids (37). Moreover, this is in agreement with recent results on MCT1, where the involvement of arginine R306 (TMH8, position 8.50) for transport activity was found, which corresponds to R445 (TMH8. position 8.50) in MCT8. In addition, on MCT1 the negatively charged residue D302 at the same TMH8 (position 8.46) was also identified to contribute in the transport mechanism (23;24;38). Guided by our MCT8 model we found on MCT8 a further charged amino acid, D498 (TMH10, position 10.49), which may cooperate with R445 in positioning the invariate L-amino acid moiety of the substrate. Consistent with an assumed substrate interaction is our observation that D498 is only conserved among MCT8 and MCT10 transporters (Fig. 1), the only MCT family members with known amino acid/iodothyronine substrates. Mutation of either amino acid to alanine entirely abrogates T_3 transport by mutant MCT8, although the mutants were exposed to the plasma membrane.

We speculate that both amino acids may bear a function beyond substrate binding. Indeed, our model suggests a salt bridge between both side-chains, which may form at least transiently during the transport cycle. Binding of substrate would cause modification of the charged interaction and in consequence break the salt bridge (R445-D498), which is possibly specific for the inward facing conformation of MCT8. In this conformation, R445 establishes simultaneously a H-bond with the backbone of TMH7 and thus constrains a triad of TMH7, TMH8 and TMH10. Destabilization at the interfaces between these helices should facilitate the assumed relative rotation of helices to each other as proposed for GlpT (20). We suggest, therefore, a dual functionality for R445 and D498 involving both substrate recognition and the molecular mechanics of transport. We did not create an R445D/D498R double mutant to test the potential salt bridge, since our model predicted that arginine at position 498 would block the presumed binding site, while an aspartate at position 445 would be to short to reach the solvent-filled channel.

We have mapped known pathogenic missense mutations in MCT8 (Tab. 2) onto our homology model and observed that some occurred around the region surrounding R445, D498, and the presumed substrate channel (Fig. 6), e.g. at D453 (TMH8, position 8.58). In the recent review of Friesema et al. (13), which was published while our work was in progress, two novel pathogenic mutations were mentioned, which are particularly pertinent to our discussion here: R445C and H192R. Both mutations have deleterious effects on T_3 transport in patients (39). According to our structural model, H192 (TMH1, position 1.66) corresponds to the substrate-binding sensitive R45 in the GlpT (20;40). Interestingly, in the crystal structure of the thyroid hormone receptor (PDB code 3GWS (41)), a positively charged amino acid is mandatory and a histidine in a T_3 binding pocket contributes to iodothyronine binding. We therefore conclude that replacement of H192 with arginine in MCT8 should potentially interfere with binding of substrate. The pathogenic substitution

R445C might lead to a loss of ionic interaction(s) consistent with our proposed mechanism for the R445A mutant. We conclude that our model can serve as a basis for further investigations into structure-function relationships in MCT8 and may further allow the rational interpretation and prediction of structural changes caused by pathogenic mutations.

REFERENCES

1. Hennemann, G., Docter, R., Friesema, E. C., de Jong, M., Krenning, E. P., and Visser, T. J. (2001) *Endocr.Rev.* **22,** 451-476
2. Abe, T., Kakyo, M., Sakagami, H., Tokui, T., Nishio, T., Tanemoto, M., Nomura, H., Hebert, S. C., Matsuno, S., Kondo, H., and Yawo, H. (1998) *J Biol.Chem.* **273,** 22395-22401
3. Friesema, E. C., Docter, R., Moerings, E. P., Verrey, F., Krenning, E. P., Hennemann, G., and Visser, T. J. (2001) *Endocrinology* **142,** 4339-4348
4. Friesema, E. C., Ganguly, S., Abdalla, A., Manning Fox, J. E., Halestrap, A. P., and Visser, T. J. (2003) *J.Biol.Chem.* **278,** 40128-40135
5. Friesema, E. C., Jansen, J., Jachtenberg, J. W., Visser, W. E., Kester, M. H., and Visser, T. J. (2008) *Mol.Endocrinol.* **22,** 1357-1369
6. Friesema, E. C., Grueters, A., Biebermann, H., Krude, H., von Moers, A., Reeser, M., Barrett, T. G., Mancilla, E. E., Svensson, J., Kester, M. H., Kuiper, G. G., Balkassmi, S., Uitterlinden, A. G., Koehrle, J., Rodien, P., Halestrap, A. P., and Visser, T. J. (2004) *Lancet* **364,** 1435-1437
7. Dumitrescu, A. M., Liao, X. H., Best, T. B., Brockmann, K., and Refetoff, S. (2004) *Am.J.Hum.Genet.* **74,** 168-175
8. Schwartz, C. E., May, M. M., Carpenter, N. J., Rogers, R. C., Martin, J., Bialer, M. G., Ward, J., Sanabria, J., Marsa, S., Lewis, J. A., Echeverri, R., Lubs, H. A., Voeller, K., Simensen, R. J., and Stevenson, R. E. (2005) *Am.J.Hum.Genet.* **77,** 41-53
9. Heuer, H., Maier, M. K., Iden, S., Mittag, J., Friesema, E. C., Visser, T. J., and Bauer, K. (2005) *Endocrinology* **146,** 1701-1706
10. Dumitrescu, A. M., Liao, X. H., Weiss, R. E., Millen, K., and Refetoff, S. (2006) *Endocrinology* **147,** 4036-4043
11. Trajkovic, M., Visser, T. J., Mittag, J., Horn, S., Lukas, J., Darras, V. M., Raivich, G., Bauer, K., and Heuer, H. (2007) *J.Clin.Invest* **117,** 627-635
12. Wirth, E. K., Roth, S., Blechschmidt, C., Holter, S. M., Becker, L., Racz, I., Zimmer, A., Klopstock, T., Gailus-Durner, V., Fuchs, H., Wurst, W., Naumann, T., Brauer, A., de Angelis, M. H., Kohrle, J., Gruters, A., and Schweizer, U. (2009) *J Neurosci.* **29,** 9439-9449
13. Friesema, E. C., Visser, W. E., and Visser, T. J. (2010) *Mol.Cell Endocrinol.*
14. Kinne, A., Roth, S., Biebermann, H., Köhrle, J., Grüters, A., and Schweizer, U. (2009) *J Mol.Endocrinol.* **43,** 263-271
15. Visser, W. E., Philp, N. J., van Dijk, T. B., Klootwijk, W., Friesema, E. C., Jansen, J., Beesley, P. W., Ianculescu, A. G., and Visser, T. J. (2009) *Endocrinology* **150,** 5163-5170
16. Biebermann, H., Ambrugger, P., Tarnow, P., von Moers, A., Schweizer, U., and Grueters, A. (2005) *Eur.J Endocrinol.* **153,** 359-366
17. Piehl, S., Heberer, T., Balizs, G., Scanlan, T. S., Smits, R., Koksch, B., and Köhrle, J. (2008) *Endocrinology* **149,** 3037-3045
18. Piehl, S., Heberer, T., Balizs, G., Scanlan, T. S., and Kohrle, J. (2008) *Rapid Commun.Mass Spectrom.* **22,** 3286-3296
19. Larkin, M. A., Blackshields, G., Brown, N. P., Chenna, R., McGettigan, P. A., McWilliam, H., Valentin, F., Wallace, I. M., Wilm, A., Lopez, R., Thompson, J. D., Gibson, T. J., and Higgins, D. G. (2007) *Bioinformatics.* **23,** 2947-2948
20. Huang, Y., Lemieux, M. J., Song, J., Auer, M., and Wang, D. N. (2003) *Science* **301,** 616-620

21. Ballesteros, J. A. and Weinstein, H. (1995) *Methods Neurosci.* **25,** 366-428
22. Salas-Burgos, A., Iserovich, P., Zuniga, F., Vera, J. C., and Fischbarg, J. (2004) *Biophys.J.* **87,** 2990-2999
23. Manoharan, C., Wilson, M. C., Sessions, R. B., and Halestrap, A. P. (2006) *Mol.Membr.Biol.* **23,** 486-498
24. Wilson, M. C., Meredith, D., Bunnun, C., Sessions, R. B., and Halestrap, A. P. (2009) *J Biol.Chem.* **284,** 20011-20021
25. Laskowski, R. A., Moss, D. S., and Thornton, J. M. (1993) *J.Mol.Biol.* **231,** 1049-1067
26. Schweizer, U., Weitzel, J. M., and Schomburg, L. (2008) *Mol.Cell Endocrinol.* **289,** 1-9
27. Scanlan, T. S., Suchland, K. L., Hart, M. E., Chiellini, G., Huang, Y., Kruzich, P. J., Frascarelli, S., Crossley, D. A., Bunzow, J. R., Ronca-Testoni, S., Lin, E. T., Hatton, D., Zucchi, R., and Grandy, D. K. (2004) *Nat.Med.* **10,** 638-642
28. Wu, S. Y., Green, W. L., Huang, W. S., Hays, M. T., and Chopra, I. J. (2005) *Thyroid* **15,** 943-958
29. Scanlan, T. S. (2009) *Endocrinology* **150,** 1108-1111
30. Ianculescu, A. G., Giacomini, K. M., and Scanlan, T. S. (2009) *Endocrinology* **150,** 1991-1999
31. Di Cosmo, C., Liao, X. H., Dumitrescu, A. M., Weiss, R. E., and Refetoff, S. (2009) *Endocrinology* **150,** 4450-4458
32. Köhrle, J. and Hesch, R. D. (1984) *Horm.Metab Res.Suppl* **14,** 42-55
33. Koehrle, J., Auf'mkolk, M., Rokos, H., Hesch, R. D., and Cody, V. (1986) *J Biol.Chem.* **261,** 11613-11622
34. Auf'mkolk, M., Koehrle, J., Hesch, R. D., and Cody, V. (1986) *J Biol.Chem.* **261,** 11623-11630
35. Wagner, R. L., Apriletti, J. W., McGrath, M. E., West, B. L., Baxter, J. D., and Fletterick, R. J. (1995) *Nature* **378,** 690-697
36. Wagner, R. L., Huber, B. R., Shiau, A. K., Kelly, A., Cunha Lima, S. T., Scanlan, T. S., Apriletti, J. W., Baxter, J. D., West, B. L., and Fletterick, R. J. (2001) *Mol.Endocrinol.* **15,** 398-410
37. Hildebrand, P. W., Rother, K., Goede, A., Preissner, R., and Frommel, C. (2005) *Biophys.J* **88,** 1970-1977
38. Halestrap, A. P. and Meredith, D. (2004) *Pflugers Arch.* **447,** 619-628
39. Capri, Y., Friesema, E. C., Touraine, R., Monnier, A., Des Portes, V., De Michele, G., Abramowicz, M., Brady, A., Vaurs-Barrière, C., Visser, T. J., and Boespflug-Tanguy, O. 2nd ELA Research Foundation Congress, Luxembourg . 2009.
40. Fann, M., Davies, A. H., Varadhachary, A., Kuroda, T., Sevier, C., Tsuchiya, T., and Maloney, P. C. (1998) *J Membr.Biol.* **164,** 187-195
41. Nascimento, A. S., Dias, S. M., Nunes, F. M., Aparicio, R., Ambrosio, A. L., Bleicher, L., Figueira, A. C., Santos, M. A., de Oliveira, N. M., Fischer, H., Togashi, M., Craievich, A. F., Garratt, R. C., Baxter, J. D., Webb, P., and Polikarpov, I. (2006) *J Mol.Biol.* **360,** 586-598
42. Jansen, J., Friesema, E. C., Kester, M. H., Schwartz, C. E., and Visser, T. J. (2008) *Endocrinology* **149,** 2184-2190
43. Vaurs-Barriere, C., Deville, M., Sarret, C., Giraud, G., des, P., V, Prats-Vinas, J. M., De Michele, G., Dan, B., Brady, A. F., Boespflug-Tanguy, O., and Touraine, R. (2009) *Ann.Neurol.* **65,** 114-118
44. Friesema, E. C., Kersseboom, S., Visser, W. E., Klootwijk, W., and Visser, T. J. ETA 2009, Lisbon . 2009.
45. Raymond, L., Whibley, A., Price, S., Rosser, E., Rahman, N., Holder, S., Stewart, F., Tarpey, P. R., Futreal, A., Stratton, M., and Gold, I. ESHG 2008, Barcelona , 60. 2008.
46. Wood, T., Hobson, D., Browning, B., Rogers, C., Skinner, C., Ardinger, C. C., Collins, C. A., Friez, M. J., and Schwartz, C. E. ESHG 2008, Barcelona , 26. 2008.
47. Namba, N., Mohri, I., Abe, S., Kitaoka, T., Miura, K., Hirai, H., Kitai, Y., Sakai, N., Taniike, M., and Ozono, K. ENDO 2009, Washington . 2009.
48. Papadimitriou, A., Dumitrescu, A. M., Papavasiliou, A., Fretzayas, A., Nicolaidou, P., and Refetoff, S. (2008) *Pediatrics* **121,** e199-e202

49. Frints, S. G., Lenzner, S., Bauters, M., Jensen, L. R., Van Esch, H., des, P., V, Moog, U., Macville, M. V., van Roozendaal, K., Schrander-Stumpel, C. T., Tzschach, A., Marynen, P., Fryns, J. P., Hamel, B., van Bokhoven, H., Chelly, J., Beldjord, C., Turner, G., Gecz, J., Moraine, C., Raynaud, M., Ropers, H. H., Froyen, G., and Kuss, A. W. (2008) *Eur.J Hum.Genet.*
50. Visser, W. E., Jansen, J., Friesema, E. C., Kester, M. H., Mancilla, E., Lundgren, J., van der Knaap, M. S., Lunsing, R. J., Brouwer, O. F., and Visser, T. J. (2009) *Hum.Mutat.* **30,** 29-38

Footnotes

The authors thank to Anja Fischbach and Antje Kretschmer, Charité, for technical assistance with LC-MS/MS experiments. Financial support was provided by Deutsche Forschungsgemeinschaft DFG, project SFB665 TP A7-2, Charité and EnForCé.

[1] The abbreviations used are: BSP, bromosulphthalein; DITPA, 3,5-diiodothyropropionic acid; ECL, extracellular loop; GlpT, Glycerol-3-phosphate transporter; GPCR, G-protein-coupled receptor; ICL, intracellular loop; IS, internal standard; LC-MS/MS, liquid chromatography-tandem mass spectrometry; MCT8, monocarboxylate transporter 8; MDCK, Madin-Darby canine kidney; MFS, major facilitator superfamily; PDB, protein data bank; SRM, selected reaction monitoring; T_3, 3,3',5-triiodo-L-thyronine; 3,3'-T_2, 3,3'-diiodo-L-thyronine; T_4, 3,3',5,5'-tetraiodo-L-thyronine, thyroxine; TAM, thyronamine; TETRAC, 3,3`,5,5`-tetraiodo-thyroacetic acid; TH thyroid hormone; TMH, transmembrane helix; TRIAC, 3,3`,5-triiodo-thyroacetic acid; TSH, thyroid stimulating hormone.

TABLES AND FIGURE LEGENDS

TABLE 1: **Device-specific liquid chromatography-tandem mass spectrometric (LC-MS/MS) parameters.** [a] (m/z): mass to charge ratio, [b] (m/z) Q1: m/z of parent ion in first quadrupole, [c] (m/z) Q3: m/z of most intensive product ion in third quadrupole, [d] DP: declustering potential (V), [e] collision energy (V), [f] collision cell exit potential (V).

TABLE 2: **Naturally occurring side-chain substitutions at the MCT8.** We extracted only those known pathogenic mutations from the literature with single side-chain substitutions (deletions or insertions are not included), because our purpose was to map the positions of such mutations to the 3-dimensional MCT8 homology model (Fig. 6) to reveal insights into their spatial neighborhood to residues R445 and D498. The mutations are helpful to evaluate function of wildtype amino acids, also with respect to their potential contact partners. Finally the combination of such sequence-structure-(mal)function relationships is a reliable procedure to identify and to describe hot-spots of transport mechanisms.

Fig. 1: Alignment of MCT subspecies. The alignment includes members of the human MCTs to extract shared and divergent features of amino acid composition. Especially conserved residues are marked in colours, according to their biophysical properties (blue - positively charged, red - negatively charged, green - hydrophobic, orange - hydrophilic, black - proline) indicating amino acids of functional or structural importance for several or all subspecies. From this alignment it becomes obvious, that the MCTs share high sequence and most likely also structural similarity, despite regions of flexibility like the third intracellular loop (ICL3). D498 of MCT8 is red boxed and can also be found in MCT10, another T_3 transporting MCT family member. Boxed are the potential dimensions of the transmembrane helices (TMHs) based on the X-ray structure of an *E.coli* Glycerol-3-phosphate transporter, another member of the major facilitator superfamily. We suggest a unifying numbering system for the MCTs indicated by the italic numbers above each TMH-box. This position identifier scheme uses a highly conserved residue in each transmembrane helix as a common reference for all members of the MCT family. For example, the highly conserved tryptophan in TMH1 is defined as 1.50 and the highly conserved proline from TMH2 is defined as 2.50. The first number is related to the particular helix, the second number after the dot determines the specific position in relation to the conserved residue. This procedure might be helpful to compare insights from different MCT species. For specific comparison between MCT subtypes we provide amino acid numbering for each MCT in the right column.

Fig. 2: Competition with ^{125}I-T_3 in uptake assays reveals essential functional groups in MCT8 substrates. *A*. Chemical structures of iodothyronines. *B-G*, MDCK1 cells were stably transfected with wildtype MCT8 and empty vector. ^{125}I-uptake of cells transfected with pcDNA3.1 was considered as background and subtracted. Uptake without inhibitor was set to 100%. ^{125}I-T_3 uptake assays with *B*, iodothyronines, *C*, D- and L-iodothyronines, *D*, thyronamines, *E*, iodothyronine derivatives, *F*, aromatic amino acids, and *G*, iodothyronine competitors.

Fig. 3: Comparison of T_3 uptake measurements based on ^{125}I-T_3 internalization or on liquid chromatography-tandem mass spectrometry (LC-MS/MS). *A.* Cell associated radioactivity depending on substrate (T_3) concentration. Lines represent fitted binding isotherms. All data points were determined in triplicate and the mean values and standard errors of the mean are indicated. The experiments were performed two times with similar results. *B*. Eadie-Hofstee plot based on data from *A*. K_M values were not approximated from the plot, but were directly calculated from the data using GraphPad software. *C*. Determination of uptake of 50 µM T_3, T_3AM, and TRIAC by wildtype MCT8 by LC-MS/MS. Data are representative of one out of at least two independent T_3 uptake experiments performed in triplicate.

Fig. 4: Homology model of the human MCT8. *A.* Crystal structure of the Glycerol-3-phosphate transporter (PDB code 1PW4, white backbone), another member of the major facilitator superfamily, which was used as a structural template. Two arginines and a histidine (blue sticks, dotted circle, GlpT amino acids R45-

TMH1, H165-TMH5, H169-TMH5, R269-TMH7) are known to be related to Glycerol-3-phosphate (G3P) binding which is mediated by the phosphate moiety of G3P (20). This binding site is located in the middle of the transmembrane region of the GlpT and is part of a central cavity which represents the presumed substrate transport channel. *B.* Lengths of specific loops and helices may vary in detail between the MCT8 model compared to the crystal structure of GlpT (*A*), but the overall topology especially in the transmembrane region is assumed to be similar. The two charged amino acids R445 in blue (TMH8) and D498 in red (TMH10) are located in the central transmembrane part of the MCT8. In the top-view with clipped extracellular loops the arrangement of the helices to each other is visualized and shows TMH8 and TMH10 in close neigborhood where these charged residues are located. Both amino acids are in close spatial distance and they are flanking the potential channel for substrate-transport (light blue circle in the top view). This spatial region superimposes with the known binding region for G3P in the GlpT (Fig. 4*A*). Therefore orientations of these residues are predestined for both helix-justification and/or substrate binding. Arginine 445 and aspartate 498 are suggested to interact via H-bond (dotted line).

Fig. 5: MCT8 surface translocation and time course of ^{125}I-T_3 uptake by MCT8 mutants R445A and D498A. *A.* MDCK1 cells were stably transfected with wildtype MCT8, R445A, D498A and empty vector. Whole cellular lysates (*left panels*) were compared by Western blotting for MCT8 with the biotinylated and affinity-purified plasma membrane protein fraction (*right panels*). Immunoblotting against β-actin was used as loading control (*bottom panles*). *B.* For time course experiments stably transfected MDCK1 cells with MCT8 mutants R445A, D498A, and empty vector were exposed to 10 nM ^{125}I-T_3 for 1 to 30 minutes. The radioactivity associated with empty vector-transfected clones was subtracted as background. Data represent of at least two independent ^{125}I-T_3 uptake experiments performed in triplicate. *C.* Determination of uptake of 50 µM T_3, T_3AM, and TRIAC by MCT8 mutants R445A and D498A by LC-MS/MS. Data are representative of one out of at least two independent T_3 uptake experiments performed in triplicate.

Fig. 6: Mapping of pathogenic side-chain substitutions onto the MCT8 homology model. We conclude from our MCT8 homology model with highlighted amino acid positions (green) of reported pathogenic side-chain substitutions (Tab. 2) that the spatial region surrounding D498 and R445 is characterized by high sensitivity for transport. The close spatial distances to amino acids like D453 or H192, which are also located at the potential transport-cavity are remarkable. However, pathogenic mutations are identified in most of the helices and some mutations may cause protein-folding defects.

TABLE 1

Compound	(m/z)[a] Q1[b]	(m/z) Q3[c]	DP[d]	CE[e]	CXP[f]
T_3	651,8	605,7	116,0	29,0	18,0
		479,0	116,0	51,0	24,0
T_3AM	607,8	590,9	116,0	23,0	20,0
		210,1	116,0	61,0	16,0
TRIAC	620,8	126,8	-15,0	-58.0	-5,0
3-T_1AM-d_4	360,0	343,1	86,0	21,0	10,0
		216,1	86,0	29,0	34,0

TABLE 2

Structural localization	Substitution	Position	References
TMH1	H192R	1.67	(39) (review (13))
TMH1	S194F	1.69	(8) (14) (42)
TMH2	G221R	2.38	(8) (43) (44)
TMH2	A224V,T	2.41	A224V: (6) (14) (42) A224T: (45)
TMH2	V235M	2.52	(8) (14) (42)
ECL2/TMH4	R271H	4.39	(14) (42) (45)
TMH4	G282C	4.50	(44) (46)
TMH5	P321L	5.59	(43)
ICL3/TMH7	G401R	7.39	(47)
ECL4	L434W		(8) (14) (42)
TMH8	R445C	8.50	(39) (review (13)
TMH8	D453V	8.58	(44)
TMH9	L471P	9.49	(6) (14) (42)
ICL5	L512P		(7) (14)
TMH11	P537L	11.49	(48) (44)
TMH12	G558D	12.54	(49) (14) (44)
TMH12	G564R	12.60	(50)
TMH12	L568P	12.64	(8) (14) (42)

Figure 1

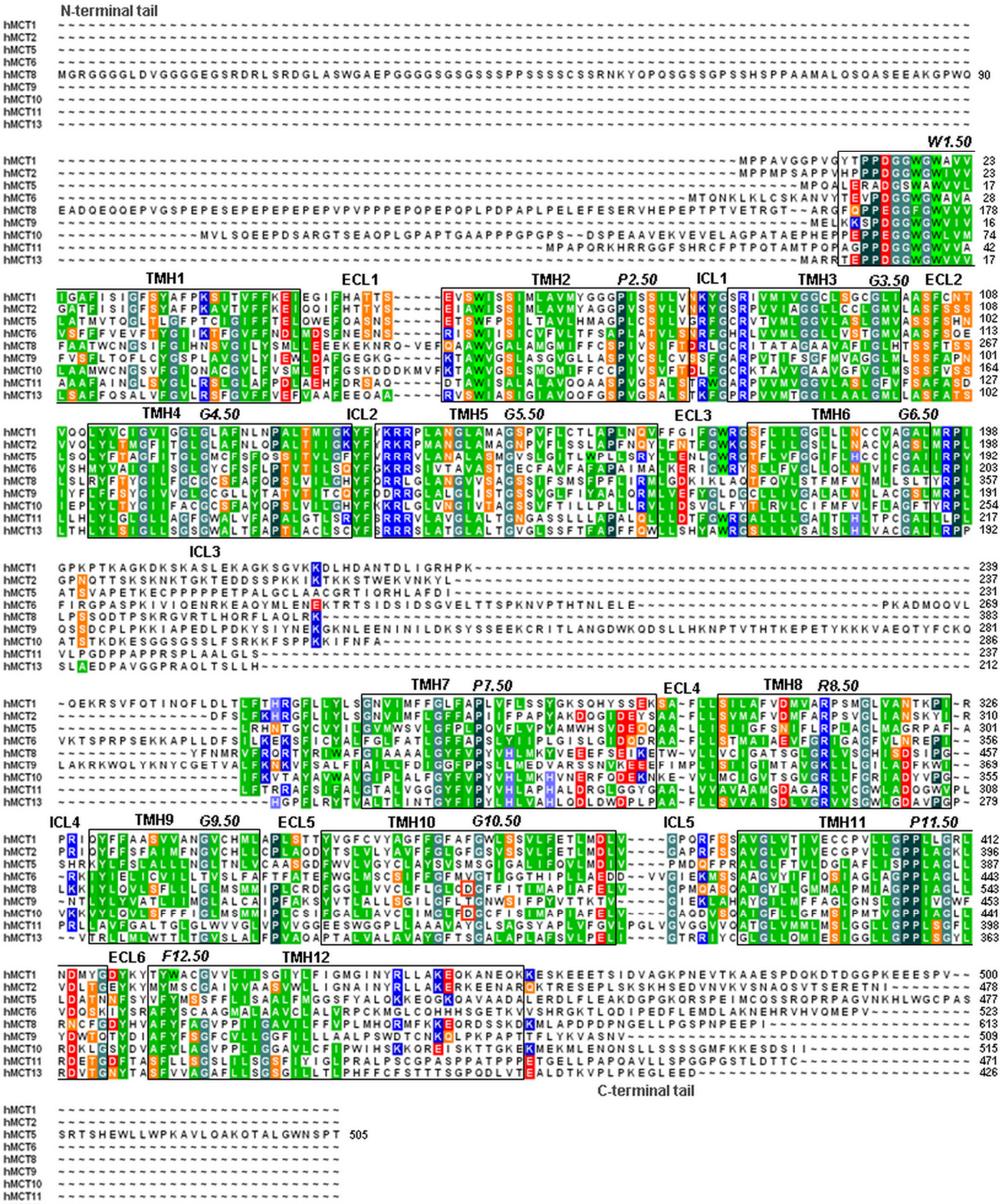

FIGURE 2

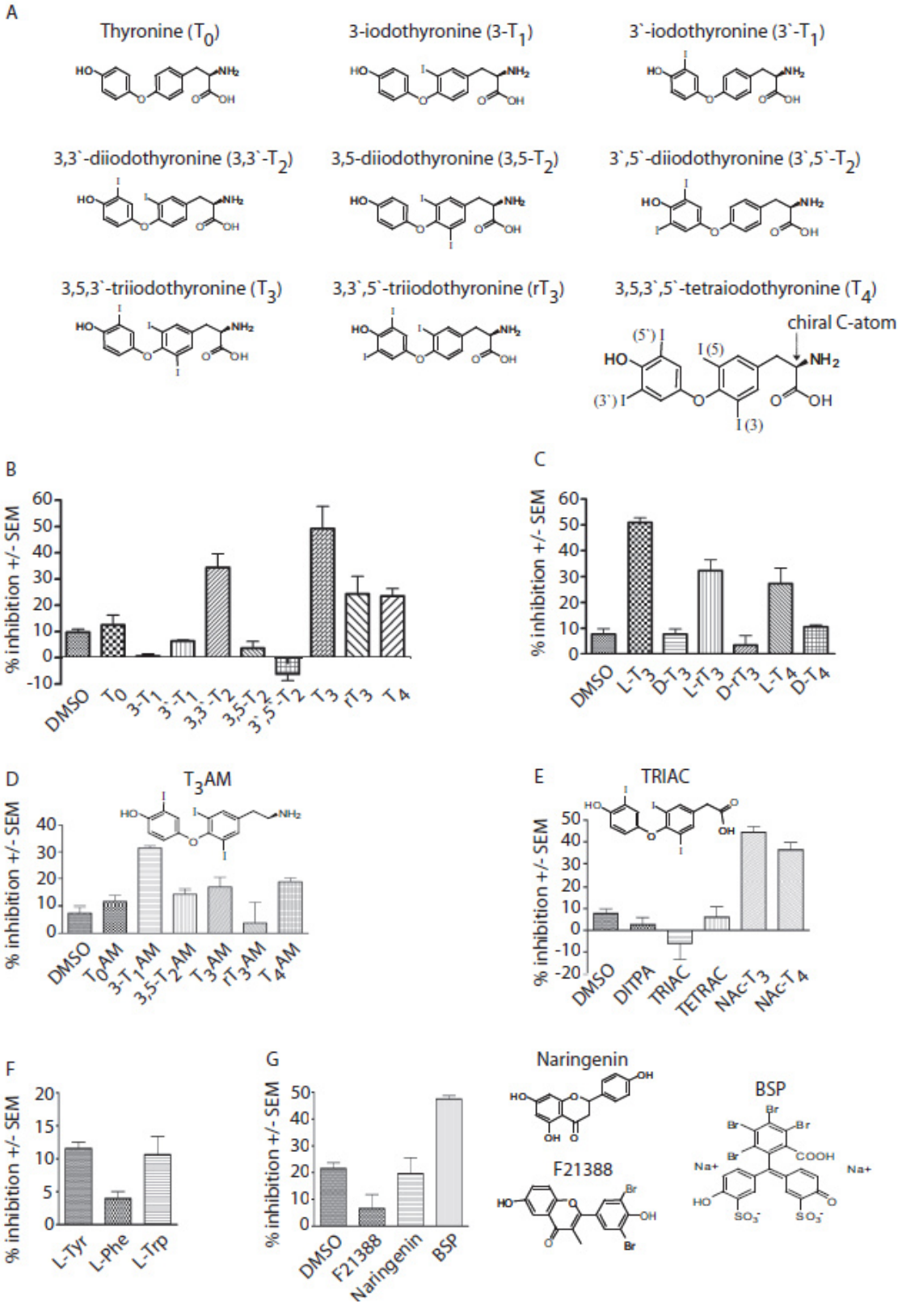

FIGURE 3

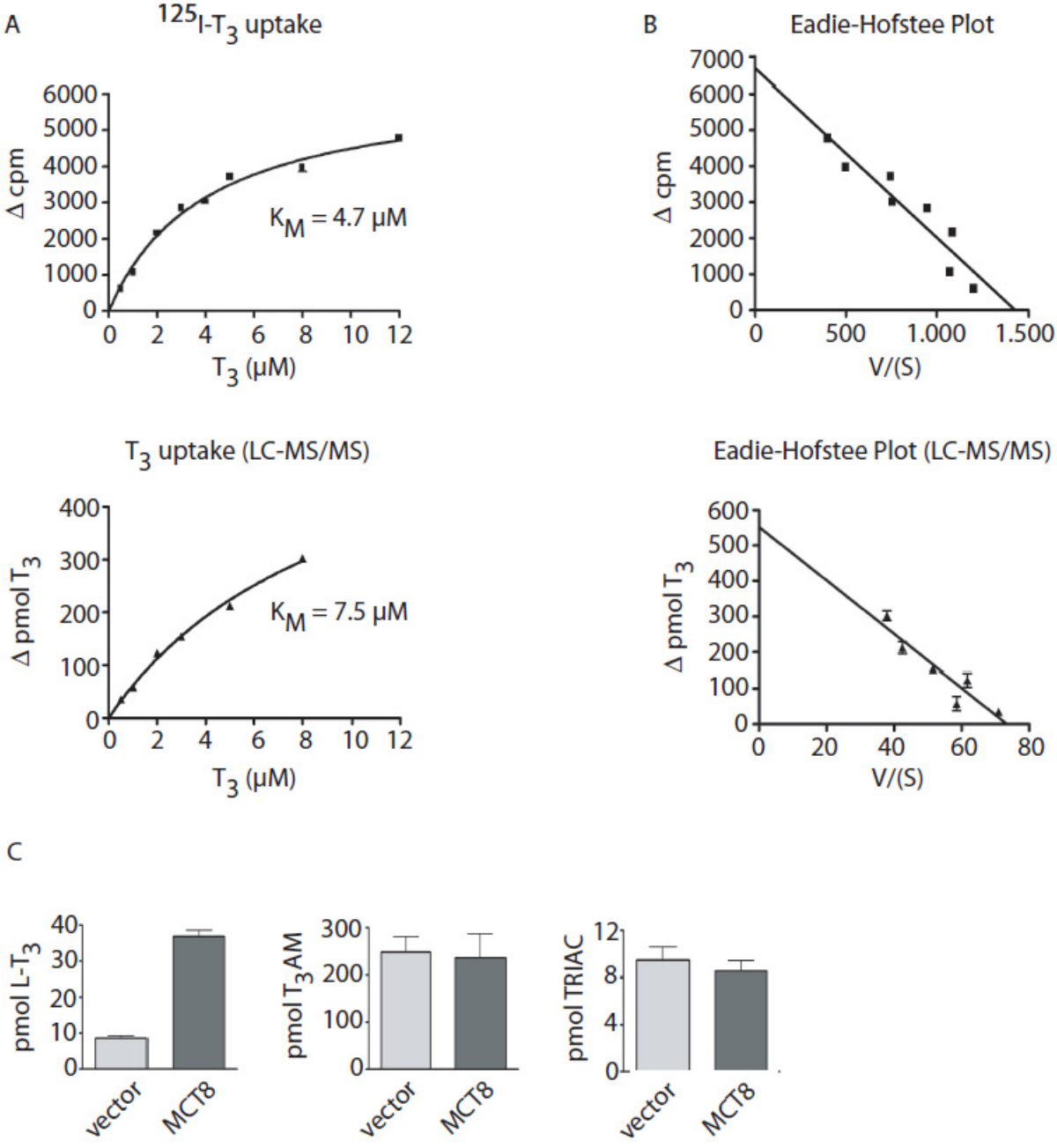

FIGURE 4

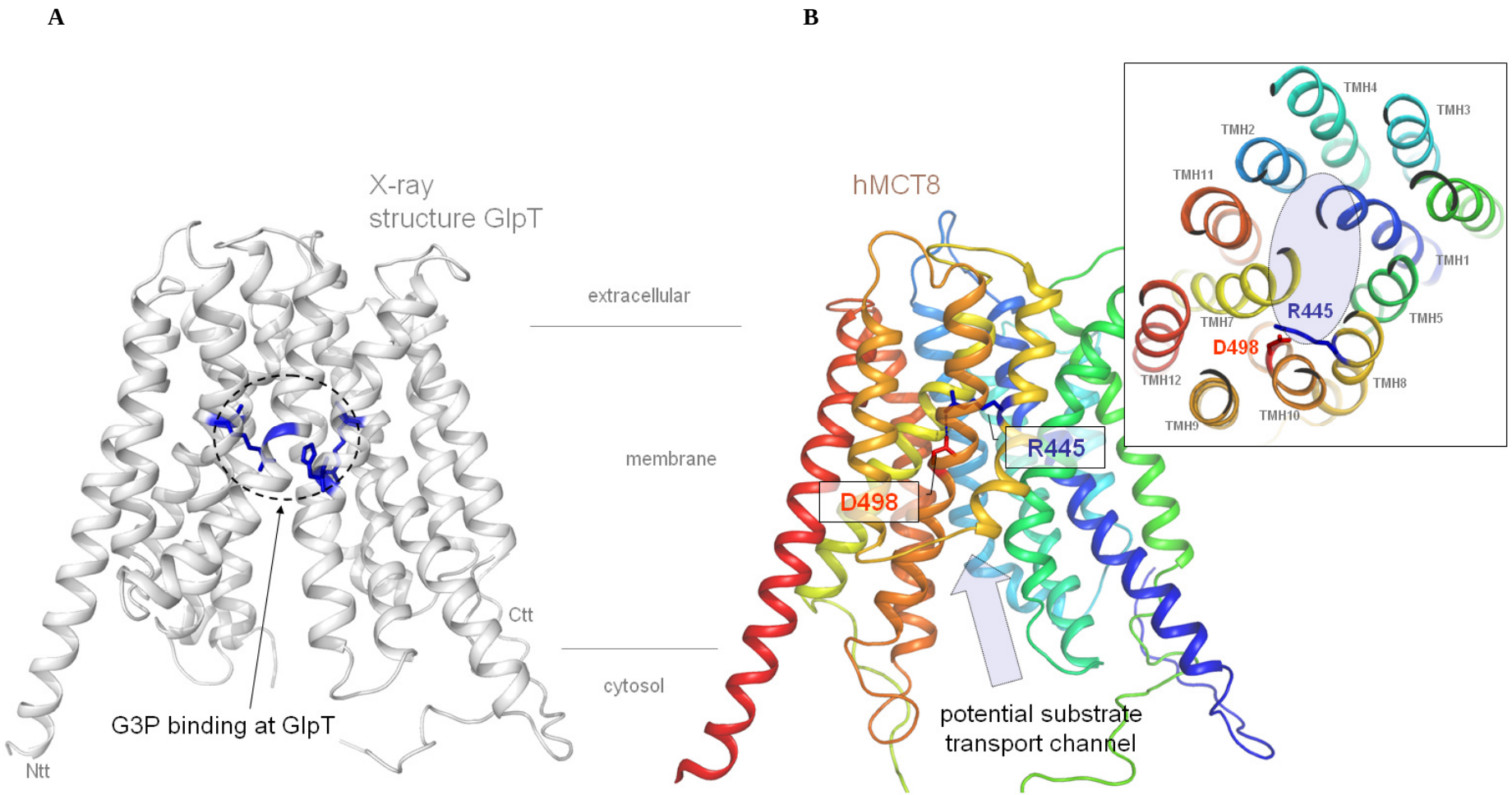

FIGURE 5

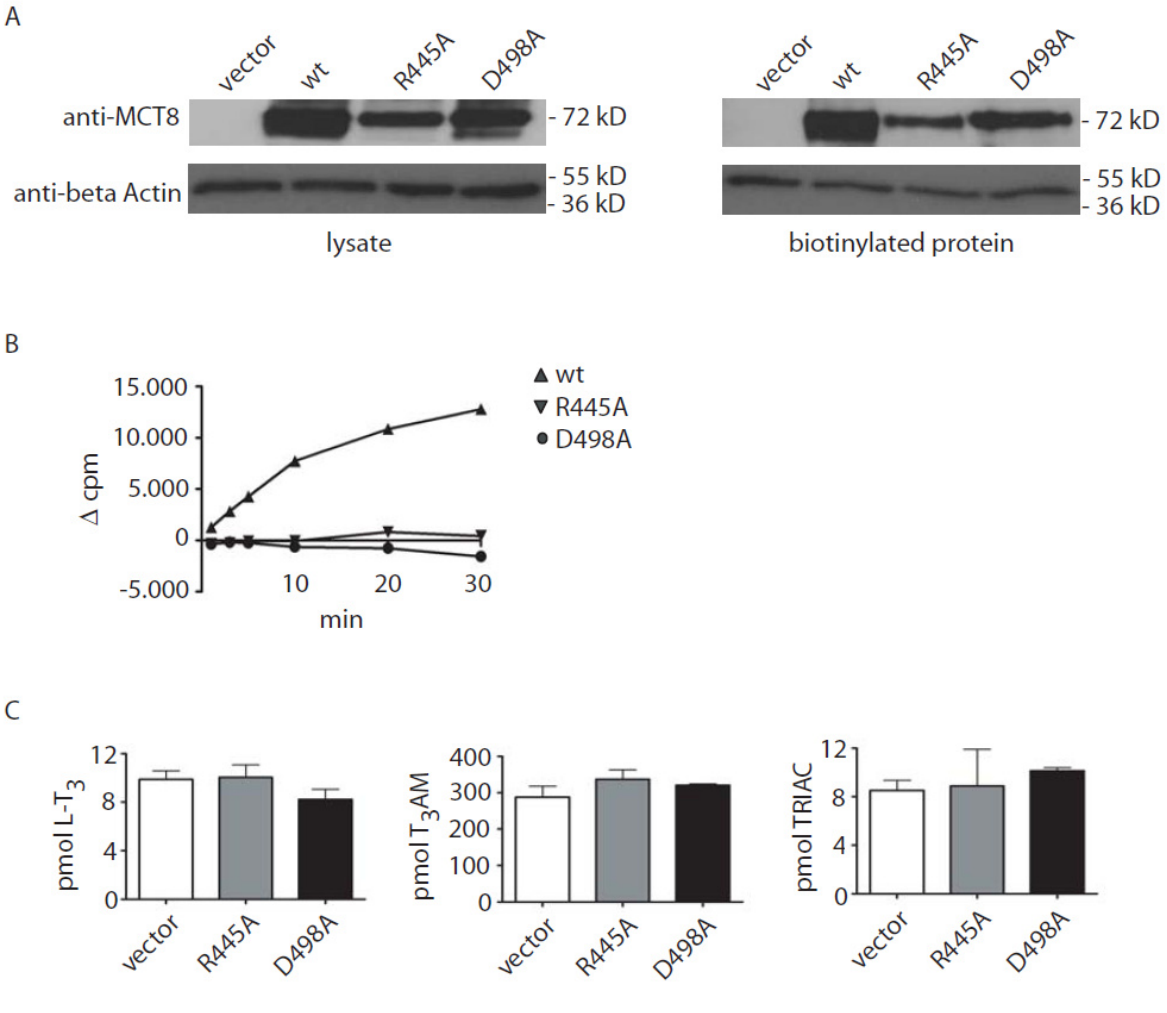

FIGURE 6